OPTICA ACTA, 1983, VOL. 30, NO. 7, 1001–1010

# Measurement of twinkling exponents of light focused by randomly rippling water

J. G. WALKER
RSRE, Great Malvern, Worcestershire WR14 3PS, England

M. V. BERRY and C. UPSTILL
H. H. Wills Physics Laboratory, University of Bristol,
Tyndall Avenue, Bristol BS8 1TL, England

(*Received 4 January 1983*)

**Abstract.** Catastrophe optics predicts that for small wavelength $\lambda$ the intensity moments $I_n$ for randomly focused light diverge as

$$I_n \sim 1/\lambda^{\nu_n}$$

and gives numerical values for the twinkling exponents $\nu_n$. We report experiments in which $\nu_n$ were obtained by comparing measurements of $I_n$ at two different wavelengths using laser light refracted by the surface of irregularly rippling water. The results support the predictions of the theory.

## 1. Introduction

When the wavelength $\lambda$ is short, optical phenomena are dominated by focusing, which typically occurs on structurally stable caustics whose forms are classified by catastrophe theory [1]. One of the striking achievements of catastrophe optics is a quantitative description of diffraction patterns near caustics. This has led to a theory [2] for the $\lambda$ dependence of the intensity fluctuations (twinkling) of random light, in terms of the normalized moments $I_n$ defined by ensemble averages over the intensity $I$:

$$I_n \equiv \frac{\langle I^n \rangle}{\langle I \rangle^n}. \tag{1}$$

The theory predicts that because of focusing the statistics of $I$ are highly non-gaussian, to the extent that the $I_n$ diverge in the following way:

$$I_n \to \frac{A_n}{\lambda_n^{\nu_n}} \quad \text{as} \quad \lambda \to 0. \tag{2}$$

Here $A_n$ are constants independent of $\lambda$ but which depend [3, 4] on the optical geometry and the statistical character of refracting or reflecting irregularities (assumed to be smooth on fine scales), and $\nu_n$ are the *twinkling exponents* which embody the main results of the theory [2] and with which this paper is concerned.

Our main purpose is to report an experimental investigation in which light of two different wavelengths is used in order to eliminate $A_n$ from measurements of $I_n$, and thus determine $\nu_n$. Randomness is introduced by passing the light through the refracting surface of irregularly rippling water, thus producing networks of

connected caustics whose geometry has been studied elsewhere [1, 5, 6, 7]. The experiment is described in § 3; the results and the way we treated them are described in § 4.

We have another purpose: to present the rather difficult theory from [2], together with some particular cases not treated explicitly there, in a simplified form more suitable for interpreting experiments. This now follows in § 2.

## 2. Catastrophe theory of twinkling

A wavefront W in the light emerging from randomly rippling water will itself be randomly curved. W is considered as a gentle deviation from a plane with coordinates $(x, y)$. If $\lambda$ is small, the light a distance $z$ beyond W is intense near caustics, which are the envelopes of the normals to W (i.e. of the rays). The light is represented by a scalar wavefunction $\psi$, which depends on $\lambda$ and on $\mathbf{r} \equiv (x, y, z)$, time $t$, and parameters $P \equiv (P_1, P_2, \ldots)$ affecting the form of W. Sometimes it is convenient to denote the *control parameters* $\mathbf{r}$, $t$ and $P$ collectively by $C \equiv (C_1, C_2, \ldots)$ and write the wave $\psi(\mathbf{r}, t, P; \lambda)$ as $\psi(C; \lambda)$.

For theoretical purposes, ensemble averages involving the intensity $I \equiv |\psi|^2$ are conveniently defined in terms of integrals over the parameters $P$, which label different members of an ensemble of wavefronts W. If W is statistically stationary with respect to spatial and temporal translation, the ensemble averages may be expressed alternatively as integrals over $(x, y)$ or $t$, leading to the following equivalent forms for the moments $I_n$ of equation (1):

*Ensemble average*

$$I_n = \frac{\int dP_1 \int dP_2 \ldots \rho(P) |\psi(C; \lambda)|^{2n}}{\left[\int dP_1 \int dP_2 \ldots \rho(P) |\psi(C; \lambda)|^2\right]^n}, \tag{3a}$$

*Space average*

$$I_n = \lim_{L \to \infty} \frac{\frac{1}{4L^2} \int_{-L}^{L} dx \int_{-L}^{L} dy \, |\psi(C; \lambda)|^{2n}}{\left[\frac{1}{4L^2} \int_{-L}^{L} dx \int_{-L}^{L} dy |\psi(C; \lambda)|^2\right]^n}, \tag{3b}$$

*Time average*

$$I_n = \lim_{T \to \infty} \frac{\frac{1}{2T} \int_{-T}^{T} dt \, |\psi(C; \lambda)|^{2n}}{\left[\frac{1}{2T} \int_{-T}^{T} dt \, |\psi(C; \lambda)|^2\right]^n}, \tag{3c}$$

where in equation (3 *a*) $\rho$ denotes the density of realizations of W in the ensemble parametrized by $P$. In most experiments, including those reported here, it is the time average (3 *c*) which is measured. $I_n$ depends on $z$ and $\lambda$; we are concerned only with the $\lambda$ dependence.

When $\lambda$ is small $I$ rises to high values on caustics, which are hypersurfaces of co-dimension 1 in $C$ space. The two-dimensional caustic surfaces observed in the

physical space **r** are sections of these hypersurfaces, resulting from a particular wavefront W at a particular time. The expressions in the numerators of equations (3 *a*), (3 *b*) and (3 *c*) are dominated by caustic sections with, respectively, constant **r**, $t$, constant $P, z, t$ and constant $P$, **r**.

Locally, each caustic is equivalent [1, 8] to one of the standard catastrophes and the wavefunction $\psi$ is described in terms of the corresponding *diffraction catastrophe* [1]. The diffraction catastrophes have great complexity of structure, but in the present context the only relevant aspect is a generalized scaling law expressing the $\lambda$ dependence:

$$\psi_j(C_i; \lambda) = \frac{1}{\lambda^{\beta_j}} \psi_j(C_i/\lambda^{\sigma_{ij}}; 1), \tag{4}$$

where $j$ labels the catastrophe (e.g.fold, cusp, elliptic umbilic) with codimension $K$ and control parameters $C_i (1 \leqslant i \leqslant K)$. In plain terms, this scaling law states firstly that at the most singular point of the caustic ($C_i = 0$) the intensity $|\psi_j|^2$ increases as $\lambda^{-2\beta}$j, and secondly that the diffraction fringes in the direction parametrized by $C_i$ shrink as $\lambda^{\sigma_{ij}}$.

We now have all the information required to calculate the $\lambda$ dependence of the contribution $I_{nj}$ of the $j$th catastrophe to the integral in the numerator of the ensemble for $I_n$ (equation (3 *a*)). Suppose the experimental arrangement is such that $N$ directions of control space can be explored. The generic case originally considered in [2] has $N = K$, but it can happen that $N < K$. This can occur in our experiments because the wavefront deformations are gentle, so that the rays are paraxial, and this in turn causes the maxima and minima of the diffraction catastrophes to be greatly elongated in the $z$ direction. In extreme cases such elongation will suppress averaging over the control parameter corresponding to $z$ while preserving averaging over parameters corresponding to variation in $x$ and $y$, which from now on we will call *transverse* directions.

The integral in equation (3 *a*) can now be estimated as

$$\begin{aligned} I_{nj} &\sim |\text{intensity at diffraction maximum}|^n \\ &\quad \times \text{hyper-volume of } N\text{-dimensional diffraction maximum} \\ &\sim \frac{1}{\lambda^{2n\beta_j}} \lambda^{\sigma_{1j} + \sigma_{2j} + \cdots \sigma_{Nj}} \\ &= \frac{1}{\lambda^{\nu_{nj}}}, \end{aligned} \tag{5}$$

where

$$\nu_{nj} \equiv 2n\beta_j - \sum_{i=1}^{N} \sigma_{ij}. \tag{6}$$

Typically, more than one type of singularity $j$ can occur, and it is obvious from equation (5) that as $\lambda \to 0$ the singularity with the largest value of $\nu_{nj}$ will dominate $I_n$. The twinkling exponents $\nu_n$ in equation (2) are therefore the victors in a competition among catastrophes, and are given by

$$\nu_n = \max_j \nu_{nj}. \tag{7}$$

To calculate $\nu_n$ it is necessary to know the numbers $\beta_j$, $\sigma_{ij}$ for all relevant singularities.

For a detailed explanation of the method of obtaining $\beta_j$ and $\nu_{ij}$ from the polynomial normal form representing the $j$th catastrophe, see [2].

The range of possibilities for $\nu_n$, as different singularities and control parameters are accessible, is illustrated by the six curves in figure 1. Each curve gives $\nu_n$ for $2 \leqslant n \leqslant 6$ (the range we studied experimentally) for a different universality class of accessible caustics, as follows.

*Curve* (*a*) is the result of competition among all catastrophes with corank 2, with all $K$ control parameters contributing to the ensemble averages. This corresponds to caustics from a two-dimensionally varying wavefront W with unrestricted randomness ($N=K$). The twinkling exponents (from [2]), followed by the dominant catastrophe(s), are

$$\left.\begin{array}{l} \nu_2=0, \quad A_2 \text{ (fold)}; \quad \nu_3=\dfrac{1}{3}, \ A_2 \text{ and } D_4 \text{ (elliptic/hyperbolic umbilics)}; \\ \nu_4=1, \quad D_4; \qquad\quad \nu_5=\dfrac{5}{3}, \ D_4 \text{ and } E_6; \quad \nu_6=\dfrac{5}{2}, \ E_6 \text{ and X}. \end{array}\right\} \tag{8}$$

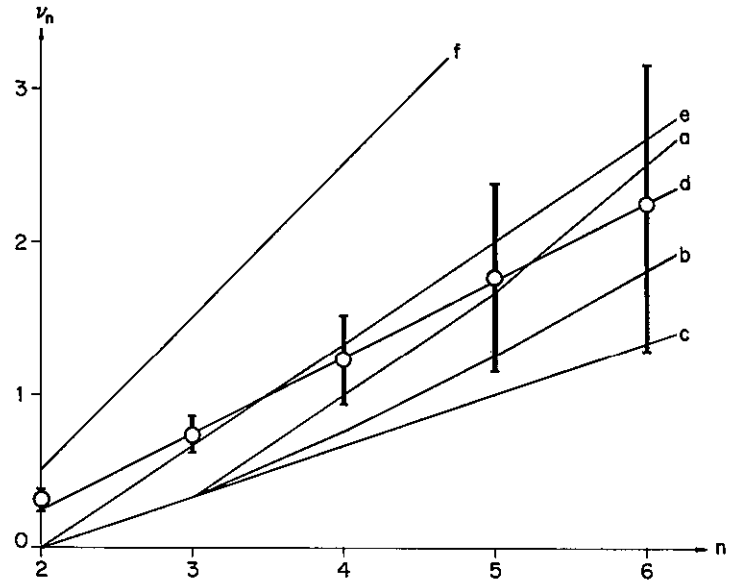


Figure 1. Theoretical and measured values of twinkling exponents $\nu_n$. Curve (*a*), exponents from generic caustics from two-dimensionally varying wavefronts; curve (*b*), exponents from generic caustics from corrugated wavefronts; curve (*c*), exponents from fold catastrophes; curve (*d*), exponents from non-generic transverse sections of cusp catastrophes; curve (*e*), exponents from non-generic transverse sections of elliptic and hyperbolic umbilic catastrophes; curve (*f*), exponents from non-generic transverse sections of $X_9$ catastrophes. The open circles represent measured exponents, with standard error bars.

*Curve* (*b*) is the result of competition among all catastrophes with corank 1 (cuspoids), corresponding to caustics from a one-dimensionally varying (corrugated) wavefront W with otherwise unrestricted randomness. The exponents are

$$\left.\begin{aligned} &\nu_2=0, \quad A_2; \qquad \nu_3=\frac{1}{3}, \quad A_2; \quad \nu_4=\frac{3}{4}, A_3 \text{ (cusp)}; \\ &\nu_5=\frac{5}{4}, \quad A_3; \qquad \nu_6=\frac{9}{5}, A_4 \text{ (swallowtail)}. \end{aligned}\right\} \tag{9}$$

The restriction to cuspoid singularities has diminished the exponents and hence the rate of divergence of the $I_n$. For this case the short-wave asymptotics of the averages in equation (3) can be fully explained [3, 4], and exact expressions for the constants $A_n$ in equation (2) can be obtained in terms of $z$ and the statistics of W.

*Curve* (*c*) gives the weakest possible twinkling exponents, which occur when only fold caustics contribute significantly to the intensity fluctuations. Then $\beta=1/6$, $N=1$ and $\sigma=2/3$, so that equation (6) gives

$$\nu_n=(n-2)/3 \quad \text{(fold)}. \tag{10}$$

*Curve* (*d*) gives the exponents corresponding to (non-generic) transverse sections through a cusp singularity: this case can occur in caustic networks [7] whenever $z$ is not too large and the observation plane $z=$constant cuts the central diffraction maximum of many cusped edges (ribs) oriented almost parallel to it, and whenever higher singularities are insignificant. Then $\beta=1/4$, $K=2$ but $N=1$ and $\sigma=3/4$, so that

$$\nu_n=\frac{n}{2}-\frac{3}{4} \quad \text{(transverse cusp section)}. \tag{11}$$

A fully worked out example of transverse cusp section dominance can be found in § 6 of [2].

*Curve* (*e*) gives the exponents corresponding to (non-generic) transverse sections through elliptic or hyperbolic umbilic singularities, which occur whenever the observation plane $z$ cuts the central diffraction maximum of many such catastrophes, and higher singularities are insignificant. Then $\beta=1/3$, $K=3$ but $N=2$ and $\sigma_1=\sigma_2=2/3$, so that

$$\nu_n=(2n-4)/3 \quad \text{(transverse umbilic section)}. \tag{12}$$

Umbilics are known to occur with diffraction patterns extremely elongated in the $z$ direction in some caustics produced by refraction at water surfaces [7, 9, 10].

*Curve* (*f*) gives the strongest twinkling exponent likely to arise in practice, corresponding to (non-generic) transverse two-dimensional sections through $X_9$ catastrophes, which are ubiquitous in caustic networks [7]. Such sections can occur in caustic junctions whose details are blurred by diffraction. Then $\beta=1/2$, $K=7$ but $N=2$ and $\sigma_1=\sigma_2=3/4$, so that

$$\nu_n=n-\frac{3}{2} \quad \text{(transverse } X_9 \text{ section)}. \tag{13}$$

We remark that the exponents $\nu_1$ predicted by equation (7) for the average intensity $\langle I\rangle$ are always negative; this means that $\langle I\rangle$ is not caustic-dominated, and

the integrals in the denominators of equations (3) play no part in the wavelength scaling. Moreover, for some cases $\nu_2$ is zero; this means that the $\lambda$ divergence of $I_2$ is weaker than the power law predicted by equation (2)—it is in fact logarithmic [2, 3, 4].

In order to determine the exponents experimentally, the coefficients $A_n$ in equation (2) must be eliminated by measuring $I_n$ at more than one wavelength $\lambda$. Ideally this is done by finding the limiting slope of a log–log plot of $I_n$ against $\lambda$, because equation (2) implies that

$$\nu_n = \lim_{\lambda \to 0} \frac{d \log I_n}{d \log (1/\lambda)}. \tag{14}$$

In practice this is not possible, and in the experiment to be described in the next section only two wavelengths, $\lambda_R$ and $\lambda_B$, were used (corresponding to red and blue light), on the assumption (justified by visual observation of well-defined caustics such as those shown in figure 3) that both wavelengths are short enough for the theory to be valid. From measurements of the corresponding moments $I_{n,R}$ and $I_{n,B}$, the twinkling exponent was calculated using the formula

$$\nu_n = \frac{\log (I_{n,B}/I_{n,R})}{\log (\lambda_R/\lambda_B)}. \tag{15}$$

## 3. Experiment

Figure 2 shows the apparatus. We used a helium–neon laser (red) operating at $\lambda_R = 0{\cdot}6238\,\mu$m and a krypton ion laser (blue) operating at $\lambda_B = 0{\cdot}4761\,\mu$m. Their beams were combined at a beam-splitter and projected through a dish of diameter 160 mm containing water to a depth of 25 mm. The ripples on the water were produced by four small dippers about 30 mm from the edge of the dish and spaced irregularly around it. Each dipper was electrically driven by an independent source of filtered random noise.

The random light waves leaving the water surface were projected on a detection plane about 4 m away. By altering the amplitude of the signals driving the dippers, a variety of random caustic networks could be produced; figure 3 shows a 1/60 s exposure photograph of a typical pattern. In the detection plane the light was divided by another beam-splitter and fell on two conjugate apertures. Interference filters

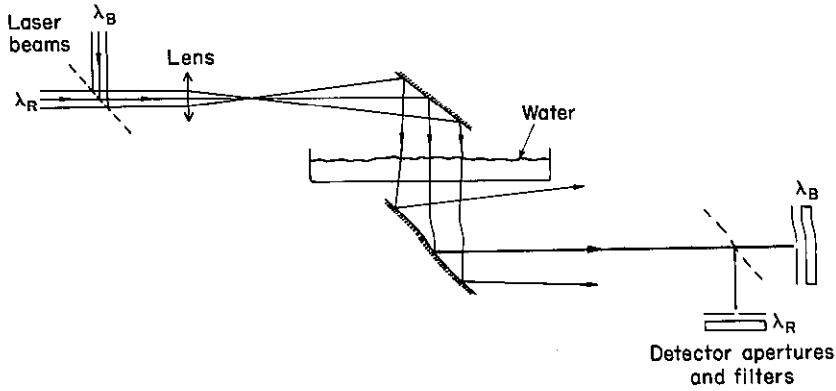


Figure 2. Diagram of experimental apparatus.

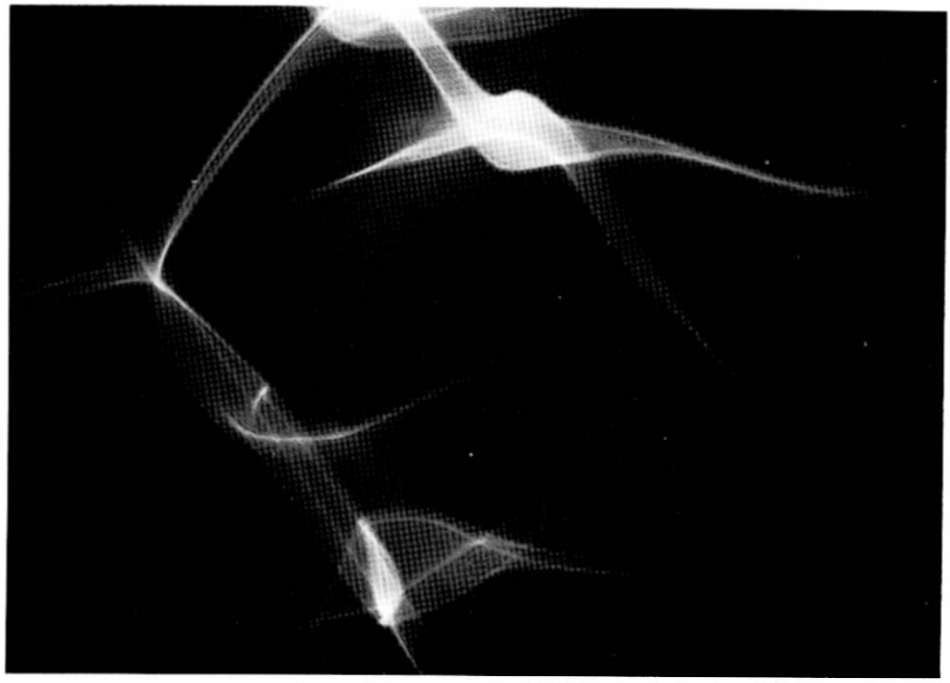

Figure 3. 1/60 s exposure photograph of moving caustic pattern typical of those whose statistics were sampled in the experiments.

behind these apertures selected the red light to fall on one photomultiplier and the blue light to fall on another, both counting photons.

Each experiment consisted of measuring the distributions $P(m, T)$ of the number $m$ of photons detected in a sample time $T$, for the red and blue channels. $T$ was 20 $\mu$s, chosen to be short in comparison with the time-scale of the shortest intensity fluctuations, which was found to be about 1 ms. Each experiment lasted 280 s, chosen to be short in comparison with the time-scale of the shortest intensity fluctuations, which was found to be about 1 ms. Each experiment lasted 280 s, chosen to exceed an estimate of the time required for moments up through the sixth to converge (J. H. Hannay, unpublished work), while being short enough for experimental conditions (e.g. laser output) to remain stable. The two photocount distributions $P_R$ and $P_B$ obtained from each experiment were used to compute the second to sixth normalized intensity moments $I_{n,R}$ according to the formula

$$I_{n,R}=\frac{\sum_{m=n}^{\infty}\frac{m!}{(m-n)!}P_R(m, T)}{\left[\sum_{m=1}^{\infty} mP_R(m, T)\right]^n}=\frac{\langle I_R^n\rangle}{\langle I_R\rangle^n}, \tag{16}$$

and similarly for $I_{n,B}$ in terms of $P_B$. Corrections were made for the dead-time of the photomultipliers and the effects of background counts.

Between 30 and 50 such experiments were conducted on each of 8 days. At the start of each day the amplitude of the signals driving the dippers was adjusted to

produce a caustic pattern with fluctuations of a given strength as measured by $I_2$, which was estimated by a preliminary run. The values of $I_2$ over the 8 days were chosen to range from 2 to 5·8, which gave fluctuations dominated by caustics but not so extreme as to make unreliable the convergence of higher moments.

## 4. Results

Because each day corresponded, in effect, to a different strength of wavefront deformation, it was decided to treat each day's data separately. Even so, the values of $I_{n,\mathrm{R}}$ or $I_{n,\mathrm{B}}$ for given $n$ varied widely among the experiments on a given day, with distributions that were grossly non-normal and highly skewed, and moreover were different from day to day.

In these circumstances it was inappropriate to represent each day's experiment by the mean values of $I_{n,\mathrm{R}}$ and $I_{n,\mathrm{B}}$, because the mean gave undue weight to (and in a few cases was essentially dominated by) experiments giving large moments. Instead we represented each day's experiments by the median values of $I_{n,\mathrm{R}}$ and $I_{n,\mathrm{B}}$, a procedure giving equal weight to all experiments (as was confirmed by the fact that the medians, unlike the means, were insensitive to the elimination of a few data).

With median values representing each of $I_{n,\mathrm{R}}$ and $I_{n,\mathrm{B}}$, the exponents $\nu_n$ for each day's experiments were calculated using equation (15). The final values were obtained as averages over the exponents for the eight days, and are shown, with standard error bars, in figure 1, superimposed on the theoretical curves discussed in § 2. It was confirmed that for each $n$ the values of the twinkling exponents were largely independent of $I_2$—that is, of the strength of the wavefront deformation. (If means rather than medians are used to represent the data, the resulting exponents are distributed about average values very close to those in figure 1 but with spreads several times greater, with the error bars for $n=5$ and $n=6$ extending to negative $\nu$.)

## 3. Discussion and conclusions

The catastrophe theory of twinkling predicts that measured exponents $\nu_n$ should lie between the extreme curves (*c*) and (*f*) in figure 1. Three non-trivial implications follow: the exponents are positive, they increase with $n$ (this does not follow from the elementary statistical fact that $I_{n+1} > I_n$ for any fluctuating function), and they are of order unity. It is clear from figure 1 that our experiments confirm all these predictions.

Examining figure 1 in detail, we see that curves (*c*) and (*f*) are incompatible with the data, consistent with visual inspection of the caustics (see figure 3) which show catastrophes of higher co-dimension than the fold and also clearly resolved internal structure in the junctions, many of which appear to be organized by $\mathrm{X}_9$. The values of $\nu_2$, $\nu_3$ and $\nu_4$ seem to rule out curve (*b*), which corresponds to generic corrugated wavefronts giving catastrophes of corank 1, and the values of $\nu_2$ and $\nu_3$ seem to rule out curve (*a*), which corresponds to generic corrugated wavefronts giving catastrophes of corank 2.

It is tempting to infer from the fact that curve (*e*)—corresponding to domination by transverse umbilic sections—lies outside the error estimate for $\nu_2$, that the data uniquely select curve (*d*)—corresponding to domination by transverse cusp sections. We resist this temptation because our experiments, using just two wavelengths, cannot distinguish the power law (2), which underlies the formula (15) on which the computation of exponents is based, from the logarithmic dependence of $I_2$ on $\lambda$

which is predicted for the cases corresponding to curves (*a*), (*b*), (*c*) and (*e*). If $I_2$ does vary logarithmically, for example as

$$I_2 \to A_2 \log \frac{X}{\lambda} \quad \text{as} \quad \lambda \to 0, \tag{17}$$

where $A_2$ and $X$ are constants, then equation (14) shows that $\nu_2 = 0$. In practice, however, equation (15) is used and yields the false exponent

$$\nu_2 = \frac{\log\left\{\log\frac{X}{\lambda_B} \Big/ \log\frac{X}{\lambda_R}\right\}}{\log\frac{\lambda_R}{\lambda_B}} \approx \frac{1}{\log_e \frac{X}{\lambda_R}}, \tag{18}$$

where the approximate form, depending only on $\lambda_R$, is valid provided that $\lambda_R \ll X\lambda_B/\lambda_R$. Not knowing the value of $X$, we are reluctant to attribute much significance to the data corresponding to $\nu_2$ in figure 1.

The above argument concerning $I_2$ illustrates the fact that our experiments involved just two wavelengths and so could not be used to test the validity of the fundamental wavelength scaling formula (2)—although they are consistent with it. The validity of this law is assumed in calculating the exponents using equation (15). It would be desirable to measure the moments for a range of wavelengths in order to test the power-law dependence directly.

We conclude by pointing out that twinkling light, whose wavelength scaling we have studied in the experiments reported here, is an example of a wider class of systems exhibiting *singularity-dominated strong fluctuations*. In light the singularities are catastrophes and the fluctuations are embodied in the intensity moments. A similar example of this sort is the semiclassical scaling (as Planck's constant vanishes) of the moments of probability density of quantum-mechanical wavefunctions associated with classical phase-space tori [11]. Another class of examples, where the singularities are also catastrophes but where the fluctuations are embodied in the universal power-law decay of a probability distribution, is exemplified by orbit periods of steady fluid motion in a plane, the amplitudes of diffracted pulses, and Van Hove singularities in spectral densities [12]. An example where the singularities are not catastrophes but convoluted lines in space is the scaling for small values of the diffusion constant of the fluctuations in concentration of pheromone in the odour plume emitted by a female insect ready for mating (M. V. Berry, unpublished work).

**Acknowledgments**

We thank Dr. J. H. Hannay and Dr. E. Jakeman for helpful discussions. One of us (C.U.) was supported by a SERC Research Fellowship.

L'optique des catastrophes prédit que, pour de courtes longueurs d'onde $\lambda$ les moments de l'intensité $I_n$, pour de la lumière focalisée d'une manière aléatoire, divergent comme: $I_n \sim 1/\lambda^{\nu_n}$ et elle donne les valeurs numériques des exposants de scintillement $\nu_n$. On présente des expériences dans lesquelles les $\nu_n$ ont été obtenus en comparant les mesures de $I_n$ à deux longueurs d'onde différentes en utilisant de la lumière laser réfractée à la surface de rides irrégulières sur l'eau. Les résultats confirment les prédictions de la théorie.

Die Katastrophenoptik sagt voraus, daß für kleine Wellenlängen $\lambda$ die Intensitätsmomente $I_n$ für zufällig fokussiertes Licht wie $I_n \sim 1/\lambda^{\nu_n}$ divergiert und gibt numerische Werte für die Funkelexponenten $\nu_n$. Wir berichten über Experimente, in welchen $\nu_n$ durch Vergleich von Messungen von $I_n$ bei zwei verschiedenen Wellenlängen mit Laserlicht erhalten wurde, welches an regellos gekräuselten Wasseroberflächen gebrochen wurde. Die Ergebnisse stützen die Voraussagen der Theorie.

## References

[1] Berry, M. V., and Upstill, C., 1980, *Progress in Optics*, Vol. XVIII, edited by E. Wolf (Amsterdam: North-Holland), pp. 257–346.
[2] Berry, M. V., 1977, *J. Phys.* A, **10,** 2061–2081.
[3] Hannay, J. H., 1982, *Optica Acta*, **29,** 1631–1650.
[4] Hannay, J. H., 1983, *J. Phys.* A, **16,** L61–L66.
[5] Berry, M. V., and Nye, J. F., 1977, *Nature, Lond.*, **267,** 34–36.
[6] Upstill, C., 1979, *Proc. R. Soc.* A, **365,** 95–104.
[7] Berry, M. V., and Upstill, C., 1983 (in preparation).
[8] Arnold, V. I., 1975, *Russ. math. Survs*, **30,** (5), 1–75.
[9] Berry, M. V., Nye, J. F., and Wright, F. J., 1979, *Phil. Trans. R. Soc.*, **291,** 453–484.
[10] Nye, J. F., 1978, *Proc. R. Soc.* A, **361,** 21–41.
[11] Berry, M. V., Hannay, J. H., and Ozorio de Almeida, A. M., 1983, *Physica* D (in the press).
[12] Berry, M. V., 1982, *J. Phys.* A, **15,** 2735–2749.